CHARACTERIZATION OF FIBER REINFORCED SHAPE MEMORY POLYMER COMPOSITE

Xin Lan*, Haibao Lv, Jinsong Leng, Shanyi Du
Center for Composite Materials and Structures, Harbin Institute of Technology, China

Keywords: *shape memory polymer, carbon fiber fabric composite, mechanical properties*

Abstract

This paper investigates the mechanical behaviors of carbon fiber fabric reinforced shape memory polymer composite (SMPC). As well-known, the major advantages of shape memory polymers (SMPs) are their extremely high strain recovery, low density and low cost, etc. However, relatively low modulus and low strength are their intrinsic drawbacks. Fiber reinforced SMPC which may overcomes the above-mentioned disadvantages is studied here. The investigation is conducted by means of four types of tests, namely, (1) dynamic mechanical analysis (DMA), (2) static three-point bending, (3) shape recovery test, and (4) optical microscopic observations of deformation mechanism at microstructural level. Results reveal that SMPC exhibits a higher glass transition temperature (T_g) and a higher storage modulus than that of pure SMP. The SMPC shows nonlinear viscoelasticity at a temperature range between T_g-20°C and T_g+20°C. At/above T_g, the shape recovery ratio of SMPC upon bending is above 90%. The shape recovery properties of SMPC become relatively stable after some packaging/deployment cycles. Additionally, the fiber micobuckling is the primary mechanism in bending of SMPC.

1 Introduction

Shape memory polymers (SMPs) are able to recover their original shape upon applying an external simulate (shape recovery effect) [1]. Among other thermal-induced SMPs, thermoplastic polyurethane-based SMP is an ordinary SMP resin with a T_g being easily tailored from -30°C to 70°C [2,3]. Thermoset epoxy-based SMP resin has also been studied in [4,5]. Styrene-based SMP is another type of thermoset SMP resin with a T_g about 80°C [6]. Thermoset cyanate-based ester SMP resin with an extremely high T_g from 135°C to 238°C has been reported recently [6]. In general, SMPs have a high strain recovery, low density and low cost [1,2]. However, pure SMPs are not suitable for many practical applications that require high strength, high stiffness, high recovery force and good resistance against creeping (e.g. actuators for deployment structures) [7]. As such, fiber reinforced shape memory polymer composites (SMPCs), such as, carbon fiber reinforced composite based on epoxy-based SMP [8,9], may be considered to meet above-mentioned requirements. Due to the excellent qualities of SMPCs, they have great potential for deployable structures, including robotics, antenna, beam and solar array in space and other applications.

In this paper, we characterize a new type of fiber reinforced styrene-based shape memory polymer composite (SMPC). Our focuses are: the basic mechanical performances, microstructural deformation mechanisms and shape recovery performances. First, the influences of fiber reinforcement on T_g as well as storage modulus are discussed. Second, the relationship between load and deflection at different temperatures is analyzed. Then, the shape recovery ratio and fiber microbuckling are studied.

2 Experimental Methods

2.1Fabrication of specimens

Carbon fiber fabric was used to reinforce a thermoset styrene-based SMP. The SMPC was fabricated by the standard fabrication techniques for fiber reinforced composite materials, i.e., curing of a pre-impregnated fabric. The SMPC was reinforced by 3-plies plain weaves. For comparison, pure SMP specimen was cured under the same conditions as that of SMPC.

2.2 Dynamic mechanical analysis

In order to investigate the basic performances of pure SMP and SMPC at different temperatures, a dynamic mechanical analyzer (NETZSCH, DMA242C) was used for a dynamic thermal scan to

determine the storage modulus and tangent delta. Three-point bending mode was applied with a span of 40 mm. The dimensions of specimens were 50×9×3 mm. The scanning range of temperature was 0~120°C at a heating rate of 2°C/min and a frequency of 1 Hz.

2.3 Three-point bending test

Instron 5569 test machine was used to investigate the basic mechanical properties of SMPC with a setup of three-point bending. The dimensions of specimens were thickness 3 mm, width 15 mm and gauge length 30 mm. The speed of crosshead was set as 2 mm/min. A thermostatic chamber (EUROTHERM 2408) was used to control the environmental temperature.

2.4 Shape recovery test

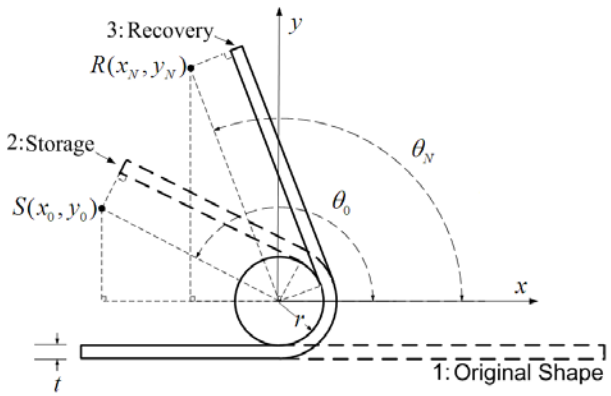

Fig. 1. Schematic illustration of shape recovery performances test

Bending test was conducted to investigate the bending recovery performances of SMPC. The method which was used to quantify the precision of deployment is illustrated in Fig. 1, where, r denotes the radius of mandrel, t represents the thickness of SMPC specimen, θ_0 is a certain original bent angle that is selected for testing, $S(x_0, y_0)$ is a point selected to determine θ_0, θ_N is the residual angle of the N^{th} thermomechanical bending cycle. $R(x_N, y_N)$ is a testing point in order to calculate θ_N:

$$\theta_N = \cot^{-1}\left(\frac{x_N}{y_N}\right) \quad (N = 1,2,3.....) \qquad (1)$$

The value of shape recovery ratio is calculated by:

$$R_N = \frac{\theta_0 - \theta_N}{\theta_0} \times 100\% \quad (N = 1,2,3.....), \qquad (2)$$

where, R_N denotes the shape recovery ratio of the N^{th} thermomechanical bending cycle.

The procedure of thermomechanical bending cycling of SMPC includes the following steps: (1) Specimen with dimensions of 80×15×3 mm was kept in water bath for 5 minutes at T_g+20°C (original shape); (2) The SMPC was bent to a certain angle around a mandrel with the radius of 2 mm in the soft rubbery state (pre-deformation); (3) The SMPC was kept in cool water with the external constraint to "freeze" the elastic deformation energy for 5 minutes (storage); (4) The SMPC specimen that was fixed on the apparatus was immersed into another water bath at a certain elevated temperature, and it recovered to a certain residual angle (recovery). Then, $R(x_N, y_N)$ was measured by a ruler with resolution of 0.02 mm. Finally, θ_N and R_N were obtained through Equations 1 and 2.

2.5 Optical microscopic observation of microstructural deformation

An optical microscope (ZEISS MC80DX) was used to observe the microstructural deformation to determine the failure mechanisms of SMPC under bending. Optical microscopic images were captured by SONY SSC-DC58AP.

3 Experimental Results and Discussions

3.1 Dynamic mechanical analysis

The curves of storage modulus and tangent delta versus temperature for pure SMP and SMPC are plotted in Fig. 2. The storage modulus of pure SMP and SMPC are 1.9 GPa and 2.6 GPa, respectively, at 24°C. According to the curves of storage modulus, it is clear that SMPC has a higher storage modulus than that of pure SMP. The storage modulus decreases sharply within the glass transition region of 40~80°C. The tangent delta curve of pure SMP approaches the peak value of 0.21 at about 54°C, while SMPC reaches the peak value of 0.47 at around 64°C. In the course of this study, the peak value of tangent delta is defined as the glass transition temperature (T_g). Hence, the T_g of pure SMP and SMPC is found to be about 54°C and 64°C, respectively. It is obvious that the T_g of SMPC is higher than that of pure SMP, which is due to the effect of fiber reinforcement. In addition, the tangent delta curve of SMPC is narrower than that of

pure SMP, which indicates that the glass transition of SMPC is faster than that of SMP.

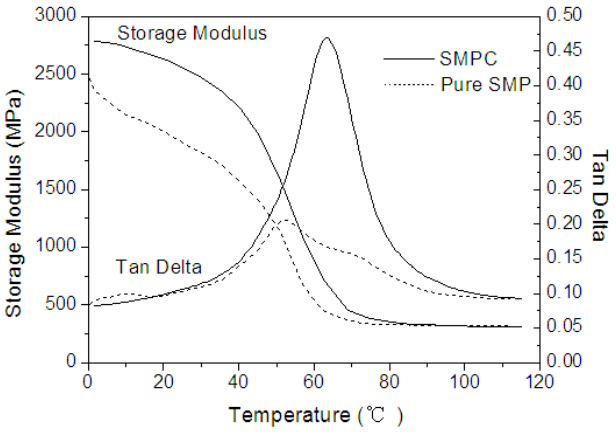

Fig. 2. Curves of storage modulus and tangent delta versus temperature of pure SMP and SMPC

3.2 Three-point bending test

In order to compare the basic mechanical properties of SMPC at different temperatures, three-point bending test was performed. Fig. 3 shows the relationship between load and deflection at some different temperatures (T_g-40°C, T_g-20°C, T_g-10°C, T_g, T_g+10°C). The results of bending modulus and maximum loads of three-point bending test at different temperatures are listed in Table 1. The bending modulus decreases remarkably with the increases of temperature associated with the softening effect due to glass transition. At T_g-40°C, SMPC exhibits the highest bending modulus than the others. In addition, at T_g-40°C, the load increased linearly to about 125.0 N with the deflection of 1.70 mm, while keeps relatively constant beyond this point. On the other hand, there is no significant linear region at testing temperatures of T_g-20°C, T_g-10°C, T_g and T_g+10°C. It is noticed that, SMPC exhibits nonlinear viscoelastic response from T_g-20°C that is the starting temperature of glass transition (Fig. 2). At T_g-10°C, the bending modulus becomes very low due to further glass transition. At T_g and T_g+10°C, the 'soft' SMP (glassy state) shows weak resistance against the applied external force.

It can be found that SMPC shows typical linear elasticity and high bending modulus before the glass transition, while exhibits apparently nonlinear viscoelasticity and low bending modulus upon the appearance of glass transition. Additionally, the results of static mechanical test coincide well with these of dynamic mechanical analysis.

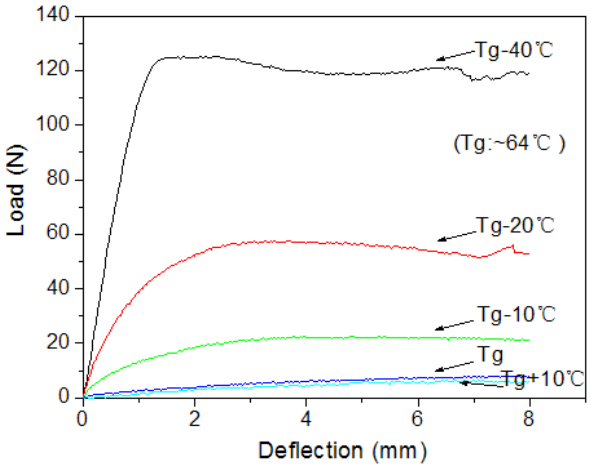

Fig. 3. Curves of load versus deflection in three-point bending (thickness: 3 mm; width: 15mm; gauge length: 48 mm)

Table 1 Properties of three point bending (T_g: ~64°C)

	E(MPa)	Maximum Load (N)
T_g-40°C	2050.9	125.0
T_g-20°C	~834.4	57.4
T_g-10°C	~293.6	22.3
T_g	~61.2	~7.6
T_g+10°C	~21.1	~6.4

3.3 Shape recovery performances

We know that carbon fiber's tensile stiffness is much higher than its compressive stiffness and the stiffness of SMP matrix at high temperature. Hence, we assume that, during bending, the neutral axis moves from the middle layer of specimen towards the outer surface where fibers are in a tensile strain state [10]. Subsequently, the traditional assumption in simple beam theory (Gere and Timoshenko, 1990) can be applied here. Based on the assumption of linear distribution of compressive strain along the thickness of specimen, one has:

$$\frac{r}{t}=\frac{1}{\varepsilon}, \qquad (3)$$

where r denotes the radius of mandrel, t represents the thickness of specimen and ε is the maximum strain on the inner surface where we assume the strain on the outer surface to be zero.

The microstructure was observed by an optical microscope after 20 thermomechanical bending cycles. In addition, the traditional material laminate can be bent to an r/t value on an order of 100. However, the SMPC laminate in this study was bent to an r/t ratio of 0.66 in order to test the recovery ratio in extremely high bending strain.

3.3.1 Shape recovery ratio at different temperatures

In order to investigate the shape recovery ratio of SMPC at different temperatures, the test of shape recovery ratio versus the number of bending cycles was conducted at some different temperatures, namely, T_g-20°C, T_g-10°C, T_g, T_g+10°C, T_g+20°C and T_g+30°C. The original bent angle was selected as 180°. The temperature of pre-deformation of SMPC was set as T_g+20°C in a water bath.

Fig. 4 shows that the recovery ratio decreases from 96% to 22% with the temperature decreasing from T_g+30°C to T_g-20°C. At T_g, the shape recovery ratio keeps within the range of 91~93%. At T_g-10°C, the shape recovery ratio decreases from 72% to 57%. At T_g-20°C, the shape recovery ratio decreases from 35% to 22%. In addition, the shape recovery effect can hardly be observed at below T_g-20°C.

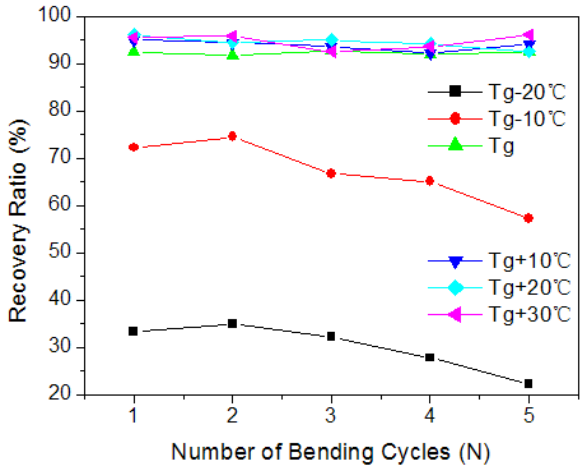

Fig. 4. Shape recovery ratio versus the number of bending cycles at different temperatures

It can be found that the shape recovery ratio of SMPC is high at/above T_g, which is above 90%. Moreover, the SMPC represents stable repeatability upon cycling. At above T_g, the shape recovery ratio against temperature shows a weak rising trend. The shape recovery behavior can also be observed within the range of T_g-20°C to T_g, which demonstrates that the glass transition occurs in a continuous region (T_g-20°C to T_g+20°C, see Fig. 2). However, the shape recovery ratio drops sharply within this temperature range due to a relatively high stiffness of SMPC at the original stage of glass transition.

3.3.2 Shape recovery ratio upon bending cycling

In order to evaluate the degradation of shape recovery, the relationship between shape recovery ratio and the number of bending cycles was tested at a bending angle of 180° at T_g+20°C (Fig. 5).

Fig. 5 shows that the recovery ratio decreases from 96% to 91% during first 50 bending cycles. For a single SMPC laminate, the shape recovery ratio decreases with a weak trend after some bending /deployment cycles. The shape recovery ratio becomes relatively stable after the 30th bending cycle, which keeps approximately at 90%. In addition, for the shape recovery process, SMPC deployed within two minutes approximately, wherein the recovery velocity in the beginning 30 seconds is relatively high.

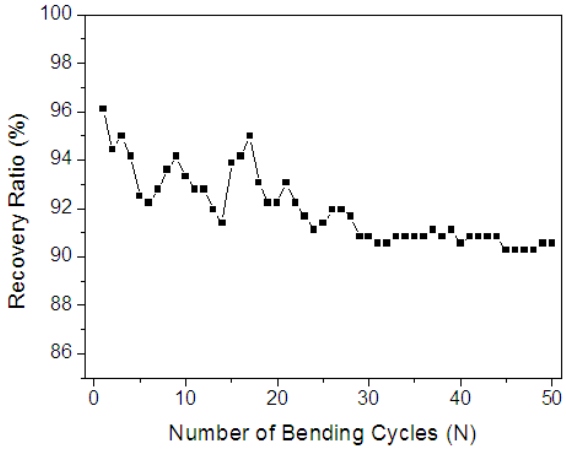

Fig. 5. Shape recovery ratio versus the number of bending cycles at T_g +20°C

3.3.3 Residual angles at different original bending angles

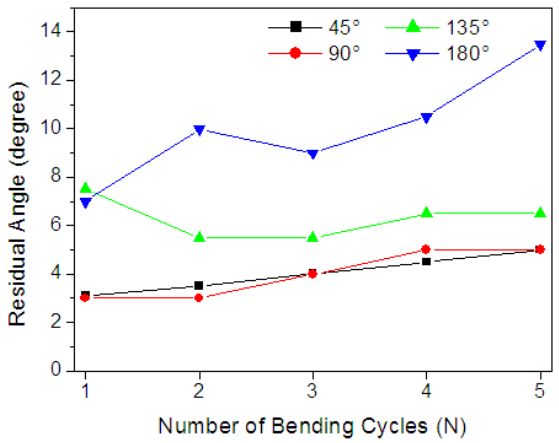

Fig. 6. Residual angle versus the number of bending cycles at different original bending angles (45°, 90°, 135°, 180°)

The relationship between residual angle in recovered configuration and the number of bending cycles was obtained at the different original bending angles of 45°, 90°, 135° and 180° (Fig. 6). Results indicate that the residual angle of the original bending angle of 45° is the lowest (3~5°). The

SMPC laminate with larger original bending angle results in a larger residual angle.

In conclusion, the shape recovery ratio under bending is primarily determined by temperature, which is high at/above T_g. Moreover, the shape memory effect can also be observed at below T_g but still within the region of glass transition, although the shape recovery ratio is low. The stability of shape recovery properties of SMPC depends strongly on the number of thermomechanical cycles. Upon bending cycling, the total instant reversible strain is deteriorated, and becomes relatively stable after sufficient numbers of packaging/deployment cycles, which is contributed by the training effect of materials.

3.4 Optical microscopic observations of microstructural deformation

The purpose is to investigate the microstructural deformation mechanism of SMPC specimens after three-point bending and numerous bending cycling.

Fig. 7 shows the optical microscopic images of SMPC specimen, which exhibits favorable combinations of fiber and matrix as well as transverse and longitudinal fiber tows before three-point bending test. Fig. 8 presents the buckled fiber fracture of transverse fiber tow on the inner surface beyond the compressive strain limit of fiber after three-point bending test. Due to the relatively high stiffness of SMP matrix at T_g-40°C, the mobility of buckled fiber in high compressive strain state is limited by the strong constraint of SMP matrix, which leads to the failure of the transverse fiber and consequently the energy dissipation. As the tensile stiffness of carbon fiber is much higher than its compressive stiffness, the neutral axis moves from the middle layer of specimen towards its outer surface where the fibers are in tensile strain state upon bending. Hence, all the other fibers that are not on the outer surface become in compressive stress state. It is also implied that the microbuckling in SMPC should be more obvious than that in an isotropic material with the same dimensions and curvature, due to the higher compressive strain on the inner surface of SMPC. In this study, the fracture of fibers on outer surface is not observed due to a 2 or 3 orders higher tensile stiffness of fiber than its compressive stiffness as well as the stiffness of SMP matrix. However, the fiber microbuckling and buckled fiber fractures on the inner surface are observed after the three-point bending test at a constant room temperature of 24°C.

Fig. 9 shows the optical microscopic images of fiber microbuckling at the bending angle of 180° after 20 thermomechanical cycles. Apparent delamination can be observed: (1) between transverse fiber tow and longitudinal fiber tow, and (2) among transverse fibers. The sinusoidal shape of fiber microbuckling of transverse fiber tow can also be observed. The wavelength of sinusoidal fiber microbuckling is about 3 mm, coinciding with the wavelength of transverse sinusoidal fiber tow. The fiber microbuckling allows SMPC to achieve an extremely high bending strain than that in traditional composites. In addition, the sinusoidal boundary of inner surface are observed, which is caused by fiber microbuckling. We also notice that the width of specimen increases and thickness decreases at the location near the mandrel due to the Possion effect in compressive strain, which is more obvious when R/t is small.

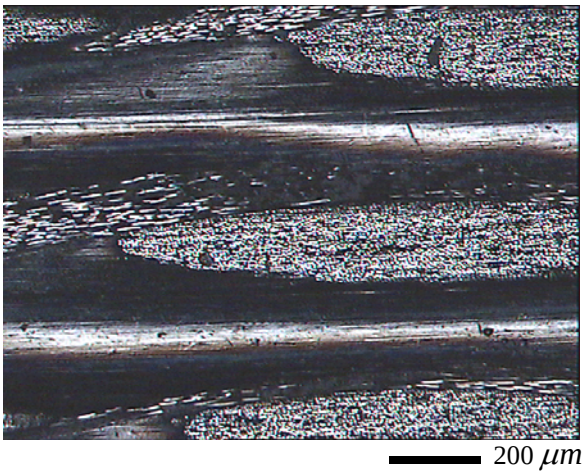

Fig. 7. Favorable combinations of carbon fiber fabric (3-plies plain weaves) and SMP matrix

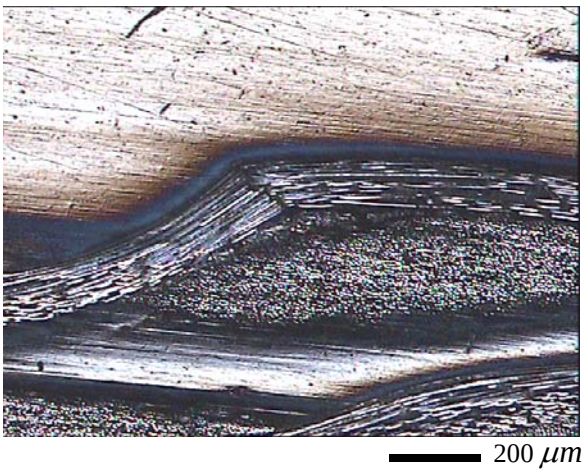

Fig. 8. Fracture of transverse fiber tow on the inner surface in high compressive stress state after three-point bending test

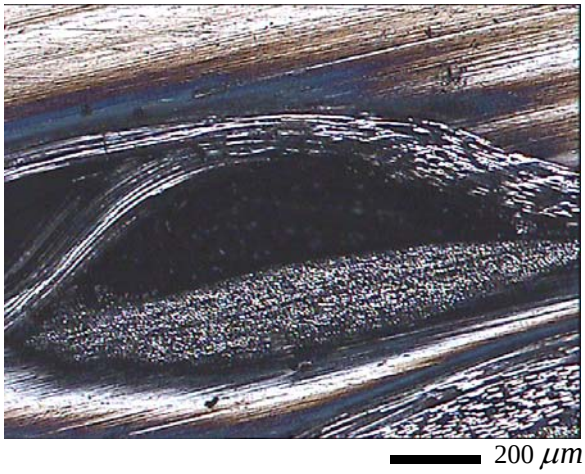

Fig. 9. Microbuckling of transverse fiber tow after 20 bending cycles

It can be concluded that both fiber fracture and microbuckling are observed in the static three-point bending test at room temperature. On contrast, only fiber microbuckling but no fiber fracture was observed during thermomechanical cycles.

4 Conclusions

In this paper, we investigate the performances of carbon fiber fabric reinforced composite based on styrene-based SMP. We may conclude that: (1) The SMPC has a higher glass transition temperature and higher storage modulus than those of pure SMP; (2) SMPC shows typical linear elasticity and high bending modulus before the glass transition in SMP, while exhibits apparent nonlinear viscoelasticity and low bending modulus within the range of glass transition in SMP. (3) The shape recovery ratio of SMPC is above 90% at/above T_g, while drops sharply at below T_g. The shape recovery properties of SMPC depend strongly on the number of thermomechanical cycles, which become relatively stable after some packaging/deployment cycles. (4) Micobuckling is the primary mechanism in the nonlinear viscoelastic bending deformation of SMPC, which provides a higher bending strain than that in traditional composite. Both fiber microbuckling and fiber fracture are observed in the static three-point bending test at room temperature. On contrast, the fiber microbuckling is obvious but fiber fracture is not during thermomechanical cycling in bending recovery test.

References

[1] Marc Behl and Andreas Lendlein, “shape memory polymers”, *Materials today*, Vol. 10, No. 4, 22-28, 2007

[2] Tobushi H, Hara H, Yamada E, Hayashi S. “Thermomechanical properties in a thin film of shape memory polymer of polyurethane series”. *Smart Materials and Structures* 5:483–91, 1996

[3] Hayashi S. “Properties and applications of polyurethane-series shape memory polymer”, *International Progress in Urethanes*, 6, 90-115,1993

[4] Yiping Liu, Ken Gall, “Thermomechanics of shape memory polymers: Uniaxial experiments and constitutive modeling”, *International Journal of Plasticity*, 22, 279-313, 2006

[5] Gall, K., Dunn, M.L., et al., “Shape memory polymer nanocomposites”. *Acta Materialia*. 50, 5115–5126, 2002

[6] Matthew C. Everhart, David M. Nickerson et al. “High-Temperature Reusable Shape Memory Polymer Mandrels”, *Smart Structures and Materials 2006: Industrial and Commercial Applications of Smart Structures Technologies*, Proc. of SPIE Vol. 6171, 61710K, 2006

[7] Ohki T, Ni QQ et al., “Creep and cyclic mechanical properties of composites based on shape memory polymer”, *Science and Engineering of Composite Materials*, 11 (2-3): 137-147, 2004

[8] Beavers, F., Gall, K., et al., “Developments in Elastic Memory Composite Materials for Spacecraft Deployable Structures”, *Presented at the 2001 IEEE Aerospace Conference*, Big Sky, MT, March 10-17, IEEE Paper No. 01-3673, 2001

[9] Abrahamson, E. R., Lake, M. S, et al. “Shape Memory Polymers for Elastic Memory Composites”, *Presented at the 43rd AIAA/ASME/ ASCE/AHS/ASC SDM Conference, April 22-25, 2002, Denver, CO*, AIAA Paper No. 2002-1562, 2002

[10] Gall, K., Mikulas, M., Munshi, N.A., “Carbon fiber reinforced shape memory polymer composites”. *Journal of Intelligent Material Systems and Structures*. 11, 877–886, 2000